Safety Concrete

Principal Investigators: Hamlin Jennings

A final report submitted to the Infrastructure Technology Institute for TEA-21 funded projects designated A458, A473, A499

DEVELOPMENT OF A FRANGIBLE CONCRETE TO REDUCE BLAST-RELATED CASUALTIES

Edward F. O'Neil, Hamlin Jennings, Jeffrey Thomas, Weiguo Shen, Toney Cummins

Biography: Edward F. O'Neil is a Concrete Materials Research Engineer for Bevilacqua Research Corporation, Huntsville, AL and formerly a research civil engineer for the US Army Engineer Research and Development Center, Vicksburg, MS. He received his BSCE from Northeastern University Boston, MA; MSCE from Purdue University West Lafayette, IN; and is currently pursuing a PhD from Northwestern University Evanston, IL. His research interests include development of very-high-strength, and high-performance concretes.

Hamlin Jennings is a Professor of Civil Engineering and Chair of the Department of Civil and Environmental Engineering. He has been with Northwestern since 1987. His research is presently focused on determining the structure of C-S-H and how it is influenced by chemistry and applied load, and to finally resolve the mechanisms of its formation (a question first posed by Le Chatelier over 100 years ago). Sensitive neutron scattering techniques are providing new information that along with completing thermodynamic data and constructing the phase diagram is providing a more complete understanding of the how the microstructure of cement-based materials develops. The microstructures of these and other materials are analyzed using an image analysis program that was developed over the last ten years to determine the principle deformations throughout the microstructure at the scale of a pixel due to forces such a drying and external load. A materials science approach is used to establish a basis for designing improved cement based materials.

Jeffrey Thomas is a Professor of Civil Engineering whose primary research interest is the atomic-level structure and microstructure of the calcium-silicate hydrate (C-S-H) gel phase that

forms during the hydration of cement-based materials. His research work with the Institute is aimed at providing concrete with properties similar to safety glass in automobiles. The purpose is to provide barrier protection while at the same time separating into very small particles in the event of an explosion, minimizing collateral damage to surrounding buildings and people.

Weiguo Shen was a visiting scholar in the NU CEE department while he worked on this project and is now a professor at the Wuhan University of Technology in Wuhan, China.

Toney Cummins is a Research Structural Engineer in the Geotechnical and Structures Laboratory, U.S. Army Engineer Research and Development Center. Mr. Cummins is actively engaged in the development of innovative blast and ballistic resistant construction materials, protective concepts, and construction criteria for both new and existing protective structures. He earned a BSCE from the University of Mississippi and his MSCE from Mississippi State University.

ABSTRACT

An investigation into the shrinkage and fracture properties of cement and slag binders was conducted along with studies on aggregate and aggregate gradation to develop a new high-performance concrete having adequate quasi-static load-bearing properties along with high frangibility under dynamic loading conditions. The purpose of this frangible concrete is to minimize casualties from large fragments of concrete propelled by a vehicle bomb detonated outside of a safety perimeter wall.

Four sets of designed experiments were executed to find the optimum mixture of slag, cement, sand, activator, water-binder ratio (w/b), aggregate to paste ratio (a/p), and curing conditions to

produce a matrix with the right level of preformed microcracks to carry a static load and to fracture under a higher dynamic load. Laboratory designed experiments measuring compressive strength and frangibility indices were followed by field blast experiments on block walls made from the frangible material to document post-blast fragment size.

Keywords: high-performance; GGBFS, dynamic loading, frangibility index, microcracking, aggregate gradation.

INTRODUCTION

Concrete is a versatile and complex building and engineering material with properties that can be significantly modified by varying its components, its curing environment, and its microstructure. When formulated for specialized characteristics such as high strength, low permeability, or light weight, such a concrete is referred to as a high-performance concrete. The American Concrete Institute[1] defines high-performance concrete as "concrete meeting special combinations of performance and uniformity requirements that cannot always be achieved routinely using conventional constituents and normal mixing, placing, and curing practices." High-performance concretes have been used in a number of studies concerning material properties. Zuber et al.[2] conducted freezing and thawing experiments using very low water/cement concretes, Punkki et al. [3] used lightweight aggregate concrete in experiments to explain composite strength. This paper describes the development of a high-performance concrete with frangible properties under dynamic blast loading that has acceptable load-carrying capacity under static loading conditions.

RESEARCH SIGNIFICANCE

Stand-off barrier walls of concrete are often used to keep vehicle bombs used by terrorists a safe distance from a target structure. But if the vehicle is detonated next to the barrier, the resulting fragments from the barrier itself are often lethal. A new specialty-designed high-performance concrete material has been developed that, under a blast force, will fracture into small pieces that may inflict injury but not kill. This material has sufficient strength under static load conditions to serve as a standoff barrier wall, and a paste microstructure that is sensitive to fracture under blast-load conditions resulting in small fragments.

BACKGROUND – PHASE 1

Acceptance criteria to judge success were established prior to developmental work. The frangible concrete would be made into precast units such as concrete masonry units (CMU's) that could be palletized and stored for use as needed. The minimum static compressive strength of the material was set at 1000 psi (6.89 MPa). The maximum size of the aggregate would necessarily be small so that fragments ejected by a blast would not be lethal. As a minimum at least 90 wt.% of the fractured particles would be required to pass a #4 sieve.

For a concrete to be weak and strong at the same time, the cementitious matrix must be strong enough to hold itself and aggregate together under a static loading environment and be weak enough to fracture into small pieces under dynamic loading stresses. An approach to achieving this state would be to design the matrix to have a built-in level of microcracking that would not be significant under the static loading regime, but would lead to significant development of microcracks under dynamic force such as a blast load. Under a dynamic load, concrete will initiate fracture along planes of weakness. Typical examples include fracture along the weak axis

of calcium hydroxide (CH) or at capillary pores in low-density calcium-silicate-hydrate (C-S-H). Initial tensile stress from the blast distributes evenly throughout the composite material. As stress rises, fractures initiate at sites of weakness. Cracks propagate with the rising stress and eventually grow together, defining the borders of uncracked fragments that are then free to leave the matrix as projectiles.

The hydration of cement based materials such as portland cement generates a variety of reaction products based primarily on calcium, silicon, and aluminum. The most important of these is a C-S-H gel that is the main binding phase in cement[4]. The C-S-H gel contains a network of fine water-filled pores that generate large shrinkage stresses as they are emptied as drying occurs, often resulting in cracking[4, 5]. Several researchers have indicated that alkali-activated ground granulated blast furnace slag (GGBFS) has a strong and generally undesirable tendency to shrink on drying [6-9] because its hydration products form little or no portlandite [4, 9-11]. Shrinkage of concrete due to loss of water, particularly at early ages, is usually undesirable; however, this shrinking and cracking is the key to successful development of frangible concrete.

Development of frangible concrete occurred in two phases. Phase 1 was designed to find the correct level of microcracking in the paste microstructure and consisted of three matrices, laboratory impact experiments, a small blast chamber experiment, and a field blast experiment. Phase 2 built on the experiments in Phase 1 and concentrated on developing the frangible concrete around the concept of ‘no-fines concrete’ adapted to a sand-sized aggregate.

EXPERIMENTAL PROCEDURES – PHASE 1

Materials and Mixtures

Three types of cementitious materials were chosen for the mixtures. The two primary materials were grade 120, GGBFS from two different plants and the third was a Type I portland cement. The activator for the GGBFS was a 2% solution of laboratory grade calcium chloride. The only aggregate in the mixture was standard “Ottawa” laboratory sand.

The experimental design for each matrix of experiments specified the amount of slag, OPC, water, additives, and sand for each mixture. The procedure for the most complex mix design (containing all ingredients) was as follows: the slag and OPC were weighed and blended dry to form the binder. The sand was weighed and added to the binder. The water was weighed and the additive thoroughly dissolved in the water. The mix water was added to the dry ingredients and the mixing continued by hand for five minutes.

Laboratory experiments

The experiments were chosen using design of experiment techniques and organized into matrices for study. For Matrix 1, eight variables were selected that were expected to influence the development of microcracks in the paste. These variables were studied with as many as three levels per variable. **Table 1** lists these variables, their levels, and comments on their choice. The experimental design optimization algorithm recommended 18 experiments be conducted to adequately study the variables and levels (**Table 2**). Cylinders, 2 in. (51-mm) in diameter by 4 in. (102-mm) long, were cast from the 18 mixtures. Compressive strength tests were conducted on the full cylinders while half-height specimens were cut for impact testing.

A blast impact was simulated in the laboratory by dropping a 14-lb (6.4 kg) steel cylinder from a height of 14 ft (4.3 m) through a tube centered over the half-sized disks, **Fig. 1**. Frangibility of the disk was determined by collecting and weighing the fragments and then sieving the pieces through a #4 sieve, weighing the passed fraction, and determining the percentage of fragments meeting the acceptable criterion. This was called the frangibility index.

The results of Matrix 1 were used to modify the input variables for the experimental design of Matrix 2. **Table 3** shows the Matrix 2 variables and **Table 4** the experimental design.

A supplemental set of the Matrix 2 mixtures was subjected to a blast force using a 4 ft (1.22 m) diameter blast chamber (**Fig. 2**) capable of directing a confined blast force of up to 100 psi (690 kPa) against a plane within the chamber. Specimens 6 in. (152 mm) square by 3/4 in. (19 mm) thick were set into frames made of 1 in. (25.4 mm) angle iron supporting the specimens on their periphery. Canisters were fastened to the underside of the frame to catch and isolate fragments of one specimen from another. These particles were collected and sieved through a set of standard sand size sieves recording percent passing each sieve. This set of experiments allowed ranking of the 18 mixtures from most to least frangible and comparison of damage from a confined blast force to damage from the drop-weight impact. Three 2 in. (51 mm) cubes from each of the Matrix 2 mixtures were tested to provide a comparison between a true and a simulated blast environment. Two of the cubes were failed in static compression while the third cube was subjected to impact loading.

The variable list for Matrix 3 built on the results of Matrix 2 and was primarily used to further test the activating effects of NaOH on the slag and to separate the effects of curing temperature and sand addition. Input parameters that were no longer varied included: the binder which was set as 100% slag number 2, the w/b set as 0.5, and the drying treatment set at 230°F (110°C) for 24 hours. Variables were the same as for Matrix 2 (**Table** 3) except that the 21-day cure time level was removed and 4-wt % NaOH included.

Field blast experiment

Based on laboratory results, frangible CMU's were fabricated and subjected to a large-scale field blast experiment. Because mass produced CMU's are demolded shortly after casting, they must be able to hold their shape and support their own weight immediately and therefore must have zero slump. Since slump was not a variable in any of the experimental design matrices, an adjustment to the best laboratory results was necessary. The s/b was raised from the range of 0 to 0.5 to a level of 5 to meet the zero-slump requirement. **Table 5** presents the field experiment mixture design.

Two wall segments were built side by side (**Fig. 3**), one of conventional CMUs and the other of frangible CMUs. Their blast-side faces were on a line perpendicular to a radial line 15.6 ft (4.75 m) from ground zero (GZ). The walls were spray painted with colors to distinguish fragments after the blast. The wall segments were constructed on a reinforced concrete footing and built three CMU's wide and ten courses high in a stack-bond fashion. The bottom two courses of each wall (not part of the blast experiment) were anchored to the concrete footing by filling their cavities with mortar to bond them to reinforcing bars that protruded from the footing. The

remaining eight courses were laid with conventional mortaring techniques. Following the blast, pieces of both walls were recovered, weighed, and distances and angles from GZ recorded using a theodolite with distance measuring equipment.

The walls were subjected to the blast effects of a simulated truck bomb by constructing a prescribed charge weight of Ammonium Nitrate and Fuel Oil (ANFO) explosive in close proximity to the wall, as might be encountered in a real world scenario. Because the walls were expected to be destroyed, they were not instrumented for pressure measurements. Rather, pressure measurements recorded on other structures, coupled with calculations performed with the ERDC-developed computer program "CONWEP"[12] were used to calculate estimates of the pressure and impulse experienced on the wall faces. The calculated peak reflected pressure was 10,470 psi and the estimated peak reflected impulse was 5423 psi-msec

RESULTS - PHASE 1

Matrix 1

The static compressive strength of the 18 experiments in Matrix 1 ranged from 498 psi (3.43 MPa) to 4996 psi (34.4 MPa) with an average of 3114 psi (21.5 MPa). Three experiments (numbers 2, 10, and 11) met both strength and frangibility requirements with average strength of 2143 psi (14.78 MPa) and average frangibility index of 97%. Adding up to 25 wt% of OPC to the slag reduced frangibility and increased strength as did increasing the s/b. Elevated curing temperature reduced strength and oven drying increased strength.

Matrix 2

Matrix 2 showed lower compressive strength and higher frangibility than Matrix 1 largely due to the use of less OPC and the reduction of sand. Also, specimens tested wet had higher strength and lower frangibility than specimens tested dry. As bound water increased, strength increased and frangibility decreased. Bound water increased with an increase in the % OPC, curing time, and curing temperature. Other results from Matrix 2 verified that the use of high slag loadings and the drying treatment are necessary for good frangibility and a small amount of OPC appears to increase the strength without greatly affecting frangibility.

Results from the small blast chamber experiment are shown in **Fig. 4** and compared to results of the drop-weight impact test for Matrix 2 samples (**Table 6**). Of the 18 slag/cement specimens in the small blast chamber experiment, 14 failed under the blast shock and 4 cracked (numbers 8, 9, 10, and 17). Data from 3 of the 14 experiments (numbers 7, 14, and 15) were lost because of metal canister failure. The blast fractured only the center portion of each panel and these were the only particles included in the analysis. Particle size gradations for the 11 successfully captured mixtures are shown in **Fig. 5**.

Field experiment of frangible block wall

A summary of the fragment data collected for fragment weights over 1 lb (0.45 kg) is in **Table 7**. The size and number of fragments from the conventional wall that could be recovered were greater than those from the frangible wall so a greater percent of the conventional wall could be recovered. **Fig. 6** shows fragment size from the frangible wall relative to the conventional wall.

Matrix 3

Strengths of Matrix 3 mixtures were very low (mean of 576 psi (3.97 MPa) after drying) and the degree of fragmentation was similar to Matrix 2. The poor strength was due to the limited degree of hydration and short curing time. Other results of interest included small doses of NaOH activator were detrimental to hydration while larger doses increased the hydration, and addition of the sand to the binder showed a modest decrease in fragmentation and had no effect on the strength.

DISCUSSION – PHASE 1

Matrices 1 - 3

At the outset of Phase 1, the notion of a strong and frangible material was just a theory and work was directed towards finding the correct paste microstructure. The Matrix 1 variables were a first attempt at setting levels to find the needed balance to achieve both frangibility and strength. The most important result from this matrix was showing that a material could be developed that had both characteristics. The fact that the mixture was too strong and not sufficiently frangible indicated that it had too much cement and possibly had been cured too long. By reducing the amount of cement to less than 10% and using the larger of the w/b, the strength would be reduced and the frangibility would be increased. This was done in Matrix 2 which had reduced static compressive strength and increased frangibility. The reduction in compressive strength was largely due to the reduced amount of OPC. The improvement in frangibility was due to two factors: the increased w/b made the paste weaker and the inclusion of sand provided many new sites for the initiation of microcracking.

Comparing the overall strength results of Matrices 2 and 3 revealed that the strength and degree of hydration were lower in Matrix 3. This is a direct result of the change in mixture design,

particularly the elimination of the 21-day hydration time. The fragmentation in Matrix 3 was on average no better than Matrix 2 despite the lower strengths in Matrix 3.

Small blast chamber

Fig. 5 shows the gradation results for the 11 experiments that were failed by the blast and whose fragment data were still valid. Three mixtures (6, 12, and 13) had the greatest mass percentage of particles passing the #4 sieve and all smaller sieves. These mixtures are highlighted in **Table 4**. All three mixtures are composed of 100% slag as binder, supporting the theory that high volumes of slag promote significant numbers of shrinkage microcracks that dictate the size of fragments produced under dynamic loading. In contrast, the majority of mixtures that did not fail or had the smallest mass passing the #4 sieve contained either 5 or 10% OPC in the mixture. The other variables in **Table 4** do not seem to correlate well to the results of this blast experiment.

Comparison of frangibility from blast and drop-weight impact

Comparisons in **Table 6** of the percentages passing the #4 sieve for each mixture reveal that in all but mixture 18 the impact test produced a larger percentage of particles meeting the 0.19 in. (4.75 mm) criterion than did the blast force. This is not completely surprising given that by standard work-energy principles a 14 lb (6.4 kg) mass dropped from a height of 14 ft (4.3 m) will impact a 2-in. (51 mm) cube with a force of 1591 lb (7078.6 N) delivering a pressure of 397 psi (2.74 MPa). By comparison, the largest measured pressure from the blast chamber was 100 psi (690 kPa). In addition, the blast pressure peaks at 100 psi (690 kPa) and then drops off while the drop weight delivers its impact and then follows with a further inertial force as the weight travels through at least one-half the height of the fractured cube before coming to rest. This latter result

prompted modification of the drop-weight impact test tube in the second phase of the developmental program.

Three of the top four mixtures (1, 2, and 4) under both force regimes were ranked the same and overall, 5 of the 11 experiments had the same ranking. These results imply that the use of a drop-weight impact loading technique is useful in predicting the results of a blast experiment of similar force.

First field blast experiment and analysis

Although the first field experiment produced results that did not meet the success criteria, the frangible concrete mixture produced fewer and smaller fragments than the conventional wall indicating that the frangible concrete concept is feasible. The major reason the frangible blocks in this field blast experiment presented less than successful results was the necessary deviation from the most successful mixture design in Matrix 3 to meet zero-slump requirements. The type of slag was changed because of availability problems; both slags were the same grade but different formulation. Different slags are affected differently[13] by type and amount of activator. Because of the change of slag, the NaOH activator was not sufficiently active to start the reaction and a sodium silicate activator was substituted. The final mixture design was sufficiently different from the recommended one that it would be difficult to predict its behavior from the laboratory fracture data.

Another explanation for unacceptable fragments of frangible block is stress redistribution. The first stress wave from a blast force is a compression wave that travels through the structure and

reflects back as a tensile wave. Initially, this tensile stress is distributed evenly to the microcracks causing weaker cracks to grow and increasing the elastic strain at stronger crack sites. As the weaker cracks grow, the stress in the stronger cracks redistributes. This process relieves stress on some microcracks and concentrates it on others, further propagating crack growth at weaker areas in preference to those where the concrete is stronger. Those cracks that are propagating join with others and define borders around stronger areas resulting in some larger fragments.

Observation of the paste matrix in a fragment of frangible block showed that the paste completely filled the spaces between the aggregate particles. This is indicative of strong concrete (minimum void space) and supports the fact that it is harder for microcracks to grow where the paste is stronger. If the voids between aggregate particles remained open, then stresses would be directed around these voids to the network of remaining connected paste. If the remaining paste were optimally designed to behave as a frangible material, it would have enough static-load-resisting strength to carry normal block wall loads but under a dynamic loading, would have a stress per unit area necessary to complete the fracture process. This observation structured the thinking for Phase 2.

BACKGROUND - PHASE 2

The mixtures developed in Phase 1 provided a cementitious paste populated with microcracks to provide frangibility. To further increase frangibility and reduce strength, a means of increasing the void space in the matrix was necessary. This would decrease strength by adding more flaws to the matrix and concentrating the external load over a smaller cross-sectional area of paste,

increasing the stress on the microcracks and encouraging more fracture sites. A promising way to increase flaws in the concrete was to adapt no-fines concrete to work with the coarse fraction of fine aggregate.

Typically no-fines concrete consists of only coarse aggregate and cement paste. It is not a new concept. It was developed in Europe in the early 20th century as an inexpensive form of concrete construction because it used a minimum volume of cement paste. Coarse aggregate would be mixed with just enough paste to form a shell around the aggregate and the coated aggregate placed in forms. During the hardening process, the paste forms a structural link to adjacent aggregate particles only at contact points providing load transfer from one point to another. Because the aggregate is mono-sized, much of the concrete volume is void space. If sand-size particles no larger than 3/16 in. (4.75 mm) can be cemented together touching neighboring particles at a small number of points, then under a blast-load the paste will fracture at the contact points breaking the matrix into particles meeting the acceptable size criteria defined at the outset.

EXPERIMENTAL PROCEDURES – PHASE 2

To optimize the composition of the mixture, a fourth matrix of experiments was conducted to study the aggregate, the aggregate gradation, the a/p, the w/b, and the process to prepare the no-fines frangible blocks. As with Phase 1, the success of the laboratory work was verified by a field blast experiment.

Materials and Mixtures

The aggregates for Matrix 4 were sand-sized materials obtained from two coarse gravel sources and one fine sand source. The particle size distributions are listed in **Table 8**. The source gravels were two kinds of < 1/4 in. (6 mm) bird's eye gravel (columns 2 and 3). The two coarse fractions (columns 4 and 5) were sieved from the source gravels and had greater than 93% of the material in the size range from 3/16 in. (4.75 mm) to 3/32 in. (2.36 mm). The fine sand fraction (column 6) was used to adjust the particle size distribution of the coarse fractions. The coarse and fine fractions were combined in different percentages to produce seven composite aggregates with different gradations.

GGBFS was used as the primary cementitious material. The chemical compositions and the properties of the slag are listed in **Table 9**. Two activating agents were used to activate the GGBFS. STAR sodium silicate solution containing 40.8% solids and a modulus of 2.51 was used as the primary slag activator. Sodium hydroxide pellets were used to adjust the modulus of the sodium silicate solution. The pellets were dissolved in water to prepare a solution with a concentration of 32.6% (Na_2O%=25%).

Table 10 shows the variables and levels used in Matrix 4. Much of the change to the no-fines concrete approach involved the choice of aggregate and the gradation. Aside from the variations in aggregate particle size distribution, three major variables were used in the design. Input parameters that were no longer varied as a result of Phase 1 studies were: the binder as 100% slag activated with 2.13% Na_2O and 3.75% SiO_2 by weight of slag, gravel aggregate 3/32 in. (2.36 mm) – 3/16 in. (4.75 mm) in size, room temperature curing conditions, and oven drying at 230 º F (110 °C) for 24 hours.

The procedure for batching the different mixtures was as follows: The slag, sodium silicate/sodium hydroxide solution and water were mixed together to make a very fluid paste. The aggregates were then added to the paste, and the material mixed until all particles were evenly coated with the paste. Cylinders 2-in. (51 mm) in diameter by 4-in. (102 mm) tall were cast from the mixtures and cured in a sealed box at room temperature for 6 days. After curing, each cylinder was sawed into one 2-in. (51 mm) diameter by 2-in. (51 mm) tall cylinder and one 2-in (51 mm) diameter by 1-in. (25.4 mm) high plate. The specimens were then dried and cooled for 24 hours before testing.

Materials property tests

Compressive strength tests were conducted on the 2 in. (51 mm) tall cylinders using a Brainard Kilman testing machine at a rank 3 loading rate. Frangibility was measured by the drop-weight impact test modified to reduce fragmentation damage. The modification was to weld nuts around the perimeter of the area where the specimen would sit (**Fig. 7**) that were just slightly shorter than the height of the specimen. The drop weight was released from a height of 39 in. (0.91 m) instead of the previous 122 in. (3.1 m). Three specimens were tested for each data point and the frangibility index recorded.

Field blast experiments

At the completion of the Phase 2 laboratory work, enough blocks were made to build a test wall for the second field blast experiment. Mixture B3 from **Table 11** was chosen as the mixture to

make the blocks because it had 100 % frangibility. The configuration of the walls was similar to the walls in **Fig. 3** from the first field blast.

As in the first experiment, the walls were subjected to the blast effects of a simulated truck bomb using a large quantity of ANFO detonated near the walls. Instrumentation and predictive techniques for pressure and impulse measurements were as for the Phase 1 blast. Due to slight variances in charge geometry and standoff range, these numbers were slightly higher than from the first experiment. The calculated peak reflected pressure was 11,960 psi and the estimated peak reflected impulse was 6042 psi-msec.

Immediately after the blast, a systematic sweep of the down-range debris field was conducted. Pieces of debris as small as 1 oz. (28 grams) were collected and documented using similar theodolite techniques as in the first blast experiment.

RESULTS – PHASE 2

Laboratory studies

The mixtures made from the components of Matrix 4 produced hardened concrete that fell into two basic categories, no-fines and dense, depending strongly on the gradation of the aggregates. The no-fines category can be further divided into two groups based on aggregate gradation, strength, and frangibility. Samples of these three groups are shown in **Fig. 8**. The binder in all groups was 100 % GGBFS.

Mixtures in no-fines group (a) had relatively low strength and very good frangibility indices. Those in no-fines group (b) had high strength and good frangibility indices. Those in the dense group (c) had high strength and low frangibility indices. These data are presented graphically in **Fig. 9**. Two mixtures tested in Matrix 4 met the requirements for strength and frangibility, with frangibility indices above 90% and strength greater than the minimum standard.

Field experiment of frangible block wall

Mixture B3 from **Table 11**, the mixture chosen to make the blocks, falls into the category of the no-fines group (a) described in **Fig. 8** above. An extreme close-up image of the surface of the frangible block is shown in **Fig. 10**. **Table 12** gives the summary of documented fragments and **Fig. 11** shows the locations of the debris.

DISCUSSION – PHASE 2

Matrix 4

The data in **Fig. 9** reveal the relationship between compressive strength and frangibility for the three groups. No-fines group (a) is tightly grouped together exhibiting the lowest strength and the highest frangibility. No-fines group (b) has somewhat higher strength and slightly lower frangibility. The dense matrix group (c) has the highest strength and lowest frangibility of all three groups as well as the most variability.

The strength and frangibility of the mixtures in all three groups is integrally tied to the particle size distribution of their aggregates. The aggregate for the no-fines (a) group is essentially a mono-sized sieving of particles that passed the #4 sieve and were retained on the #8 sieve. Since

the aggregate particles are essentially uniform in size, the number of point-to-point contact locations between pieces of aggregate will be close to the minimum. The cement paste that forms at the contact locations is the only physical structure holding the aggregate together. Thus the stress on the cross-sectional area of the cement at a contact point will be high given that the number of contact points will be low.

The aggregate gradation for a specimen in group (b) contains particles of two sizes, 80 % the same as group (a) and 20% passing the #8 sieve. The better particle packing of aggregate develops more point-to-point contacts between aggregate particles and higher strength and lower frangibility as a function of greater area of paste at structural contact points.

The specimens in group (c) have the highest particle packing efficiency. The small particles and fine sand further fill void spaces, create more point-to-point contact points, and evenly distribute the cement paste making the mixture denser, stronger, and much less frangible.

Referring to **Fig. 9**, group (b) specimens performed the best with respect to both strength and frangibility. However, there are a small number of group (c) specimens that have the same frangibility as group (b) but lower strength. Why the group (b) specimens can have higher strength and the same frangibility as some of the group (c) specimens can be explained by studying the specimen fragment morphology. **Fig. 12** shows the fragment morphology of group (b) and group (c) specimens with similar frangibility (91.23%, 90.47% respectively). Group (b) specimens broke into particles with diameters mainly in the 3/16- to 3/32-in. (4.75 to 2.36 mm)

range while the group (c) specimens mainly broke into very fine size particles < 3/32 in. (2.36 mm).

Craus and Ishai[14] assumed that the specific surface of all particles having a sphere or a cube shape could be expressed by the equation

$$S = \frac{6}{\rho \cdot D} \tag{1}$$

where S = Specific surface, ρ = Particle density, and D = Particle diameter. This says the specific surface of a particle decreases as the particle diameter increases, so the fragments of no-fines concrete have a much smaller specific surface area than the dense concrete. This implies that a smaller new surface increment results from the fracture of no-fines concrete than from the dense concrete when those two kinds of concrete break into pieces with a similar mass of particles smaller than 3/16 in. (4.75 mm). From Griffith - Orowan - Irwin failure criteria, for a crack to propagate it needs a certain amount of energy of fracture. The crack propagation forms new surface area in the body resulting in the reduction of strain in the surrounding area and the corresponding release of elastic energy from the body[15, 16]. This energy of fracture can be described by equation 2

$$\delta_\tau = G \cdot \delta_S \tag{2}$$

where δ_τ = the energy of fracture necessary to form the new fracture surface area, G = the energy released into the crack tip per unit area of the crack (the elastic strain energy release rate), and δ_S = the new surface area created by the crack growth.

For those samples of group (b) and dense group (c) having the same frangibility and experiencing the same dynamic impact energy, their main difference is that the dense concrete has a much higher surface increment and a much lower elastic strain energy release rate, *G*. Since the dense concrete is a quasi-brittle material, the strain energy release rate can be represented by equation (3)[17, 18]

$$G = 2(\gamma_s + \gamma_p) \tag{3}$$

where G = the strain energy release rate, γ_s = the specific surface energy, and γ_p = the plastic deformation energy associated with crack extension. So while it has the same frangibility as the no-fines group (b) specimens, the dense concrete has a lower sum of plastic deformation energy, γ_p, and specific surface energy, γ_s. Thus it has weak bonding among the particles before fracturing and is easier to fracture, so it has lower strength than the no-fines group (b) concrete.

Second field blast experiment and analysis

From the post-blast fragment collection, the pieces that could be found were the large ones that did not break up. There were 7 such pieces of the no-fines frangible wall that weighed greater than 1 oz. (28 grams). However, the largest of these fragments was ineligible as it was part of a grouted foundation block. The largest piece that did qualify had a mass of 4 oz. (113 grams). The mass of eligible fragments collected was 15 oz. (425 grams) or 0.07 % of the 1350 lb (612.5 kg) mass of the entire wall. In contrast, 59 pieces were recovered from the conventional wall that had a mass greater than 1 oz. (28 grams). The largest piece from this wall had a mass of 2.31 lb (1.05

kg) and the mass of all eligible fragments collected was 35.9 lb (16.3 kg) or 3.52 % of the wall. The collected pieces of fragments from both walls are shown in **Fig. 13**.

The six eligible fragments of frangible concrete constituted a very small percentage of the whole wall. The percentage of the wall that did break up into fragments less than 0.19 in (4.75 mm) is not known because the evidence was too small to find. However, the fact that no more than seven deficient pieces could be found is strong evidence that a large fraction of the remainder did meet the criteria. Close-up examination of these pieces revealed excess paste in the spaces between aggregate particles. This paste filled many of the void spaces creating a denser, stronger matrix making the concrete more difficult to fracture. This condition underlines the importance of accurately proportioning the a/p and keeping the paste rheology stiff enough that over vibration will not cause excessive flow.

Two mixtures from Matrix 4 had acceptable strength and frangibility (**Table 11**). Mixture B3 was chosen because its frangibility index was 100 %. Its strength was just within the acceptable level which made it more susceptible to dynamic force than the higher strength mixture B1. Had mixture B1 been used to make the blocks, it is speculated that there would have been more fragments not meeting the minimum criteria.

The interrelationship between strength and frangibility raises an important question. What are the optimum proportions to use given that both strength and frangibility are important? Knowing that frangibility and strength are, to some extent, inversely proportional, what amount of strength should be sacrificed to increase the frangibility? High frangibility and low strength make

conditions for excellent small-sized blast debris but poor load carrying capacity. On the other hand, compromising frangibility for excellent strength defeats the original purpose as well. Within the scope of the mixtures developed in this program to make a high-performance frangible concrete, it has been demonstrated that very high frangibility indices accompany very low strengths and that very high strength concretes produce low frangibility indices. But it has also been shown that high frangibility indices can be accompanied by moderately high strength, mixture B1 is an example. While mixture B3 performed very well in the role of frangible concrete when compared to conventional block, its strength performance was on the poor end of acceptable. A more appropriate solution would use a mixture designed for a slightly lower frangibility index with a compressive strength greater than Mixture B3 but lower than mixture B1.

CONCLUSIONS

The laboratory experimental work and field testing to develop frangible concrete took place over the span of six years. During that time four experimental matrices of laboratory-developmental experiments were conducted augmented by one small-scale confined blast-load experiment and two full scale field-blast-load experiments against frangible-concrete- and conventional-concrete-block walls. From this work the following conclusions can be made:

1. The results from the static compressive strength experiments, the drop-weight impact experiments, and the full-scale field blast experiment of Phase 1 revealed that overall, the compressive strength exceeded expected levels and the frangibility of specimens was less than what was expected. While the results from this phase were not on the mark, they showed that properties of strength and frangibility were not mutually exclusive and proper adjustment of component materials can bring the desired properties inline.

2. Use of alkali-activated GGBFS as a cementitious material under proper curing and heat treating will produce a matrix of shrinkage microcracks throughout the fabric of the cement paste that will withstand moderate quasi-static loads, yet complete the fracture process producing small blast debris fragments under dynamic blast loading conditions.
3. Based on the frangibility rankings of a matrix of 18 slag/cement concrete mixtures fractured by both a drop-weight impact tester and a confined blast-load environment producing peak pressures of approximately 100 psi (690 kPa), it can be said that the drop-weight impact tester, modified as described in this paper, can be a reasonable substitute for a confined blast-load test of the peak pressures described above.
4. The developmental approach to producing frangible concrete in Phase 2 focused on the concept of no-fines concrete and the efforts to adapt that technology to a sand-size aggregate source. From the results of static and dynamic experiments on sand-size aggregates of seven different gradations coated with a slag binder, it is concluded that:
    a. a mono-sized aggregate produces a material with too few structural contact points having very low static strength but excellent frangibility,
    b. a poly-sized gradation of three or more sizes produces a material with too many structural contact points that has excellent strength but a very low frangibility index,
    c. the optimal gradation lies between these two extremes and involves a dual sized aggregate gradation that incorporates some particle packing to increase the contact points and the strength yet only sacrifices a small amount of frangibility.
5. The results of the field blast experiment in Phase 2 revealed that the fragmentation of the frangible concrete wall was significantly better than the conventional block wall. The

mass data of the frangible wall presented in **Table 12** are between 38 and 50 times smaller than data for the conventional wall. Two of the Matrix 4 mixtures, one of which was used to make the blocks in the Phase 2 blast experiment, met the strength and frangibility guidelines set up as a measure of success, From these data it is concluded that frangible concrete, made using no-fines principles applied to sand-size aggregate, while not perfect is a successful solution to finding a concrete that will minimize fatalities from blast fragment debris.

ACKNOWLEDGMENT

The authors would like to acknowledge the long-term support of the Geotechnical and Structures Laboratory of the U.S. Army Engineer Research and Development Center who funded this work and who conducted both field blast experiments, and Dr. Jean O'Neil for editorial support.

REFERENCES

1. ACI Committee 116, "Cement and Concrete Terminology", *ACI Manual of Concrete Practice, Part 1, Materials and General Properties of Concrete.* American Concrete Institute, Farmington Hills, MI, Revised Annually

2. Zuber, B., Marchand, J., Delagrave, A., and Bournazel, J. P., "Ice Formation Mechanisms in Normal and High-Performance Concrete Mixtures", *Journal of Materials in Civil Engineering, ASCE,* 12, no. 1, Feb. 2000, pp 16-23.

3. Punkki, J., Gjorv, O.E., and Monteiro, P. J. M., "Microstructure of High-Strength Lightweight Aggregate Concrete" in *4th International Symposium on Utilization of High-Strength/High-Performance Concrete,* F de Larrard, and R Lacroix, eds., Laboratoire Central des Ponts et Chaussees: Presses de l'ecole nationale des ponts et chaussees, 1996, pp 1281-87.

4. Taylor, H. F. W., *Cement Chemistry*. 2nd ed., Thomas Telford, London, England, 1997.

5. Jennings, H. M., "Colloid Model of C-S-H and Implication to the Problem of Creep and Shrinkage", *Materials and Structures / Concrete Science and Engineering,* V. 37, No. 1, 2004, pp 59-70.

6. Richardson, I. G., "The Nature of the Hydration Products in Hardened Cement Pastes", *Cement & Concrete Composites,* V. 22, No. 1, 2000, pp 97-113.

7. Collins, F., and Sanjayan, J. G., "Cracking Tendency of Alkali-Activated Slag Concrete Subjected to Restrained Shrinkage", *Cement and Concrete Research,* V. 30, No. 4, 2000, pp 791-98.

8. Wang, S., Pu, X., Scrivener, K. L., and Pratt, P. L., "Alkali-Activated Slag Cement and Concrete: a Review of Properties and Problems", *Advances in Cement Research,* V. 27, No. 7, 1995, pp 93-102.

9. Wang, S. D., and Scrivener, K. L., "Hydration Products of Alkali Activated Slag Cement", *Cement and Concrete Research,* V. 25, No. 3, 1995, pp 561-71.

10. Brough, A. R., and Atkinson, A., "Sodium-Silicate-Based, Alkali-Activated Slag Mortars Part I: Strength, Hydration and Microstructure", *Cement and Concrete Research,* V. 32, 2002, pp 865-79.

11. Roy, D. M., and Idorn, G. M., "Hydration, Structure, and Properties of Blast Furnace Slag Cements, Mortars, and Concrete", *ACI Materials Journal,* V.. 73, No. 12, 1982, pp 444-57.

12. Hyde, D. W., "CONWEP, conventional weapons effects software, v 2.1.0.1", U.S. Army Engineer Research and Development Center, Vicksburg, MS, 2004.

13. Cincotto, M. A., Melo, A. A., and Repette, W. L., "Effect of Different Activators Type and Dosages and Relation to Autogenous Shrinkage of Activated Blast Furnace Slag Cement", *Proceedings of the 11th International Congress on the Chemistry of Cement: Cement's*

Contribution to the Development in the 21st Century, G. Grieve, and G. Owens, eds., Document Transformation Technologies, 2003, pp 1878-87.

14. Craus, J., and Ishai, I., "Method for the Determination of the Surface Area of Fine Aggregate in Bituminous Mixtures", *Journal of Testing & Evaluation,* V. 5, No. 4, 1977, pp 284-91.

15. AASHTO, *Standard Specification for SuperPave Volumetric Mix Design*, AASHTO Designation MP 2-99, AASHTO, 1999.

16. Broek, D., *Elementary Engineering Fracture Mechanics*, Kluwer Academic Publishers Group, 1982.

17. Portela A., *Dual Boundary Element Analysis of Crack Growth.* Computational Mechanics Publications, 1993.

18. Barsom, J. M., and Rolfe, S. M., *Fracture and Fatigue Control in Structures,* American Society for Testing and Materials, West Conshohocken, PA, 1938.

TABLES AND FIGURES

List of Tables:

List of Figures:

Table 1–Type and levels of variables in the Matrix 1 experiments

Variable	Levels	Comments
% portland cement (OPC)	0, 10, and 25 %	Remainder of binder is slag
Type of slag	1 or 2	Slags were grade 120
Sand-binder ratio (s/b)	0 and 0.5	Sand may have an important effect on failure mode
Water-binder ratio (w/b)	0.35 and 0.5	A low and high w/b would make a stiff or liquid paste
Chemical activator	Either none or 2% $CaCl_2$	$CaCl_2$ is known to increase OPC drying shrinkage
Curing time	7 and 28 days	Longer curing promotes more hydration and greater strength
Curing temperature	68 and 140 °F (20 and 60 °C)	To test temperature effects on drying shrinkage.
Drying treatment	24 hr at 230 °F (110 °C) or 50% RH at 68 ° F (20 °C)	Does speed of drying affect shrinkage?

Table 2–Experimental design for Matrix 1

Experiment number	% OPC	Slag type	Sand/ binder	w/c	$CaCl_2$ activator used	Cure time, days	Cure temp, °F (°C)	Drying treatment*
1	0	1	0	0.35	yes	28	68 (20)	1
2	0	1	0	0.5	no	28	140 (60)	2
3	0	1	0.5	0.5	yes	7	68 (20)	1
4	10	1	0	0.35	no	7	140 (60)	1
5	10	1	0.5	0.5	no	28	68 (20)	1
6	10	1	0.5	0.35	yes	28	140 (60)	2
7	25	1	0	0.5	yes	7	140 (60)	2
8	25	1	0.5	0.5	no	7	68 (20)	2
9	0	2	0	0.35	no	28	68 (20)	2
10	0	2	0	0.5	no	7	68 (20)	1
11	0	2	0.5	0.5	no	7	140 (60)	2
12	0	2	0.5	0.35	yes	7	140 (60)	1
13	10	2	0	0.35	yes	7	68 (20)	2
14	10	2	0	0.5	yes	28	140 (60)	1
15	10	2	0.5	0.5	yes	28	68 (20)	2
16	25	2	0	0.5	no	7	140 (60)	1
17	25	2	0.5	0.35	no	28	140 (60)	1
18	25	2	0.5	0.5	no	7	68 (20)	2

* 1 = drying 24 hrs at 230 °F (110 °C); 2 = drying to equilibrium at 50% RH and 68° F (20 °C)

Table 3–Type and levels of variables in the Matrix 2 experiments

Variable	Levels	Comments
% OPC	0, 5, and 10 %	Mass of cement reduced by 250 % from Matrix 1

Type of sand	Coarse, fine	Average size of coarse sand = 3/32 in. (2.36 mm), fine sand = 3/64 in. (1.1 mm)
Sand-binder ratio	0, 0.12, and 0.25	Sand may have an important effect on failure mode
Chemical activator	Either none or 2% NaOH	$CaCl_2$ only accelerates OPC. NaOH accelerates slag hydration
Curing time	3, 7 and 21 days	Adding 3 days will tell if short cure is enough
Curing temperature	68, 140, and 176 °F (20, 60, and 80 °C)	To test non-linear temperature effects on drying shrinkage.

Table 4–Experimental design for Matrix 2

Experiment number	% OPC	Sand/binder ratio	Sand type	NaOH activator	Cure temp. ° F (°C)	Cure time (days)
1	10	0.25	coarse	2%	176 (80)	21
2	5	0.25	fine	2%	176 (80)	21
3	0	0.12	coarse	2%	140 (60)	21
4	5	0.12	coarse	No	140 (60)	21
5	10	0	n/a	2%	68 (20)	21
6	0	0	n/a	No	68 (20)	21
7	5	0.25	fine	No	176 (80)	7
8	10	0.25	coarse	No	176 (80)	7
9	5	0.12	coarse	2%	140 (60)	7
10	0	0.12	fine	No	140 (60)	7
11	10	0	n/a	2%	68 (20)	7
12	0	0	n/a	2%	68 (20)	7
13	0	0.25	coarse	2%	176 (80)	3
14	0	0.25	fine	No	176 (80)	3
15	10	0.12	coarse	No	140 (60)	3
16	10	0.12	fine	2%	140 (60)	3
17	5	0	n/a	2%	68 (20)	3
18	5	0	n/a	No	68 (20)	3

Table 5–Mixture design used to make frangible block in the first field blast experiment

% Slag	S/b	W/b	Activator	Cure temp	Dry temp
100	5	0.5	2.13% Na_2O and 3.75% SiO_2	5 days at 68° F (20°C)	230° F (110 °C) for 24 hours

Table 6–Ranking of fragments from blast and impact experiments

Gradation Analysis Ranking	Mixture number (% particles passing the #4 sieve)	
	Blast	Impact
1	6 (70.7)	6 (96.9)
2	13 (63.4)	13 (80.7)
3	12 (62.2)	5 (75.9)
4	3 (40.8)	3 (73.9)
5	11 (32.9)	12 (67.5)
6	18 (27.9)	4 (57.9)
7	16 (25.1)	16 (49.6)
8	4 (24.2)	11 (41.2)
9	5 (21.9)	1 (34.7)
10	2 (14.6)	2 (31.6)
11	1 (8.6)	18 (26.0]

Table 7–Summary of fragment data collected from first field blast

Wall	Number of fragments	Mass range, lb (kg)	Average mass, lb (kg)	Total mass found, lb (kg)	Percent of total wall
Conventional	74	1-13, (0.45-5.9)	2.73 (1.24)	217.58, (98.9)	40.01
Frangible	47	1-3.96, (0.45-1.8)	2.08 (0.94)	96.36, (43.8)	14.31

Table 8–Particle size distribution for source and sieved aggregates

Sieve opening, in. (mm)	Source gravel, % passing		Sieved gravel, % passing		Sand, % passing
	Source 1	Source 2	Sieved 1	Sieved 2	
0.374 (9.5)	100	100	-	-	-
0.187 (4.75)	90.08	85.43	100	100	100
0.093 (2.36)	24.96	21.40	27.71	25.30	97.85
0.046 (1.18)	6.02	3.50	6.68	4.14	89.40
0.024 (0.6)	3.36	0.80	3.73	0.95	76.35
0.012 (0.3)	1.77	0.38	1.96	0.45	38.50
0.006 (0.15)	1.08	0.12	1.20	0.14	15.45
0.003 (0.075)	0.47	0.08	0.52	0.10	3.60

Table 9–Chemical composition of slag

Compound	GGBFS, %
CaO	37.2
SiO_2	34.2
Al_2O_3	9.5
Fe_2O_3	0.7

SO_3	2.6
MgO	10.7
Alkali Na_2O	0.1

Table 10–Type and levels of variables in the Matrix 4 experiments

Variable	Levels	Comments
w/b	0.4, 0.45	w/b must make paste stiff enough to cling to aggregate
a/p	2.6, 3.1, 3.6	Aggregate to paste ratio must be such that there is just enough paste to coat the aggregate.
Cure time, days	3, 7	At temperature of 68˚F (20˚C)

Table 11–Properties of frangible concrete mixtures chosen for block fabrication

Mixture	a/p	w/b	Activator dosage, %	Weight ratio of sodium silicate	Setting speed	Dry strength, MPa	Frangibility %
B1	3.8	0.45	4.5	0.8	Normal	22.67	94.5
B3	3.8	0.45	6.0	1.8	Fast	7.54	100

Table 12–Summary of fragment data collected from second field blast

Wall	Number of fragments	Mass range, lb (kg)	Average mass, lb (kg)	Total mass found, lb (kg)	Percent of total wall
Conventional	59	0.062 – 2.31 (0.028 – 1.049)	0.608 (0.276)	35.93 (16.301)	3.52
Frangible	6	0.062 – 0.249 (0.028 – 0.113	0.016 (0.071)	0.94 (0.425)	0.07

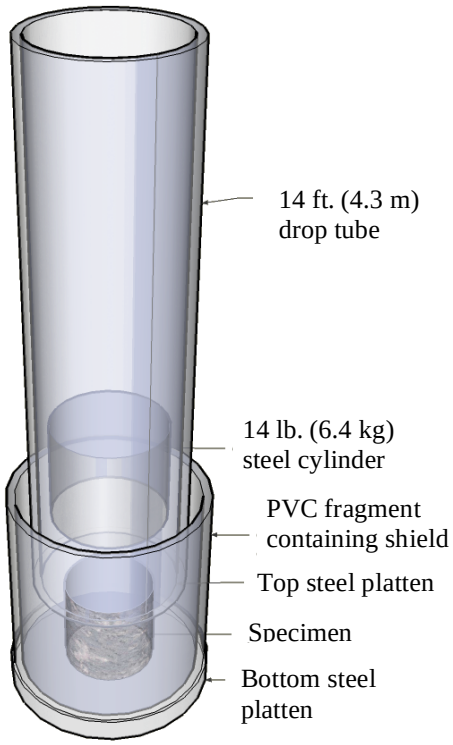

Fig. 1–Drop-weight tube.

Fig. 2–Four-foot (1.22-m) blast chamber.

Fig. 3–Test walls ready for field blast experiment.

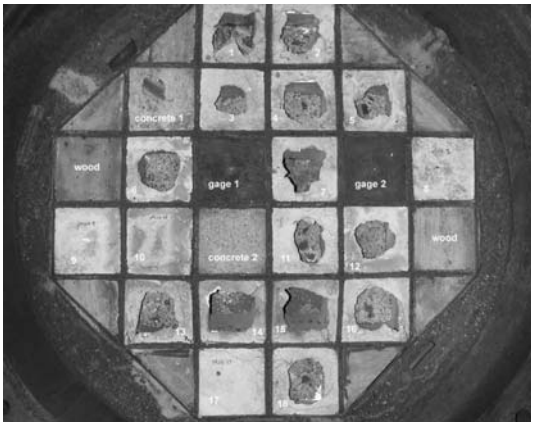

Fig. 4–View of failed blast chamber panels.

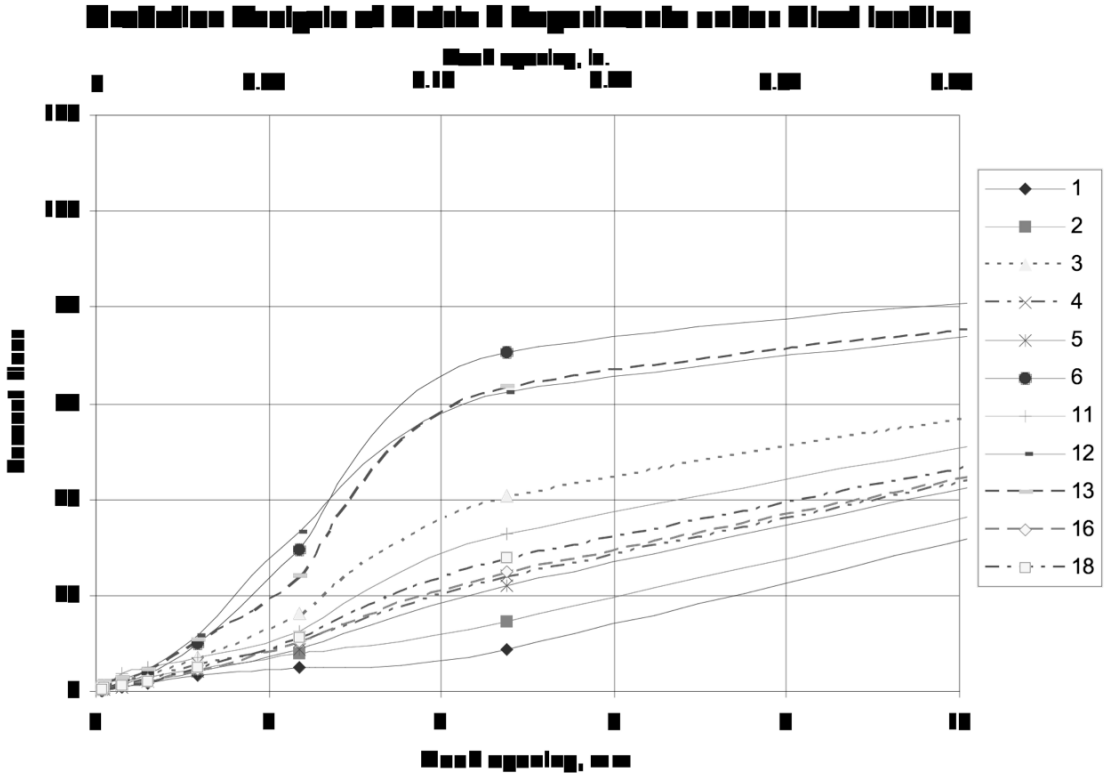

Fig. 5–Sieve analysis of 11 surviving blast chamber experiments.

Fig. 6–Fragments from the first field blast: frangible wall left, conventional wall right.

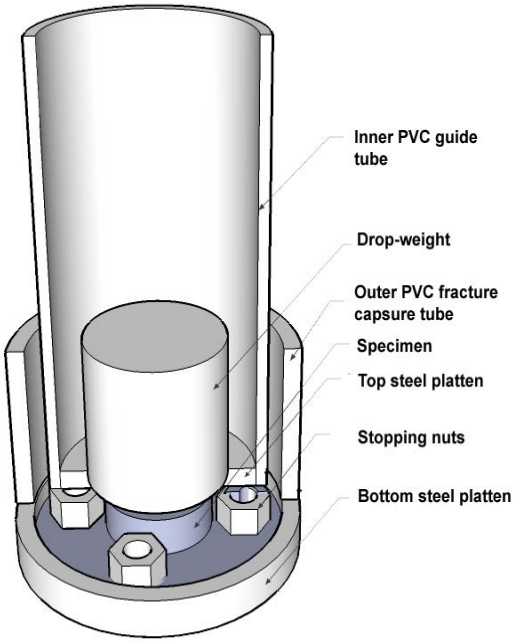

Fig. 7–Cut section of drop-weight tube with modification.

Fig. 8–Samples of the groups of frangible concrete with different gradation aggregate. (a) 3/16-3/32 in. (4.75-2.36 mm) aggregate, (b) aggregate with 80% of 3/16-3/32 in. (4.75-2.36 mm) and 20% of 3/32 in.-pan (2.36-0 mm), (c) aggregate with 65% of 3/16-3/32 in. (4.75-2.36 mm) and 20% of 3/32 in.-pan (2.36-0 mm), and 15% of fine sand.

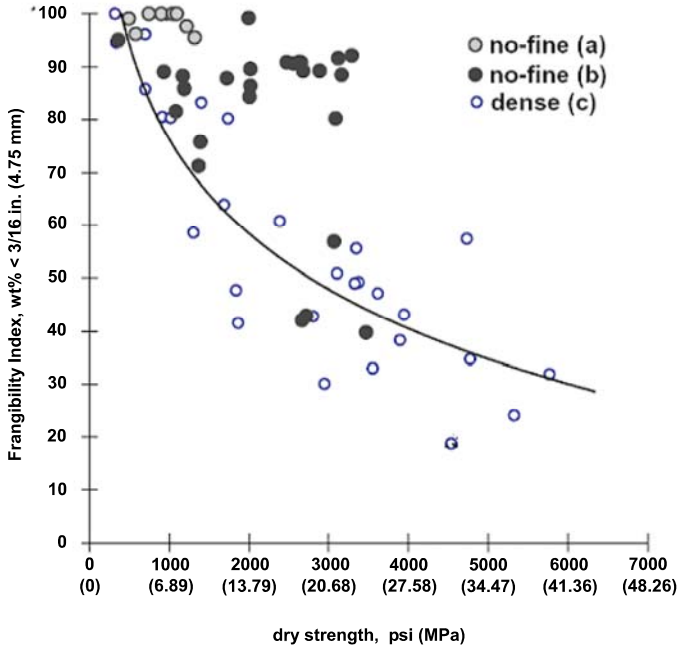

Fig. 9–Relationship between compressive strength and frangibility index.

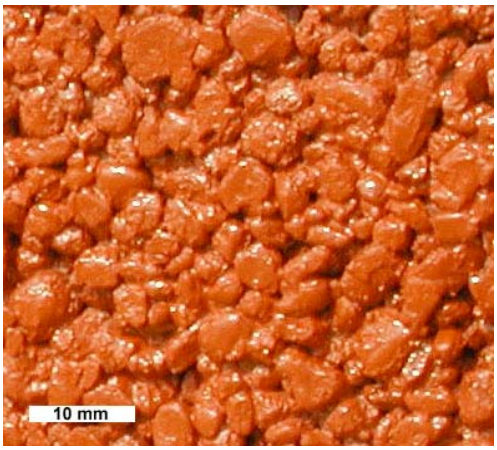

Fig. 10–Close-up of frangible block.

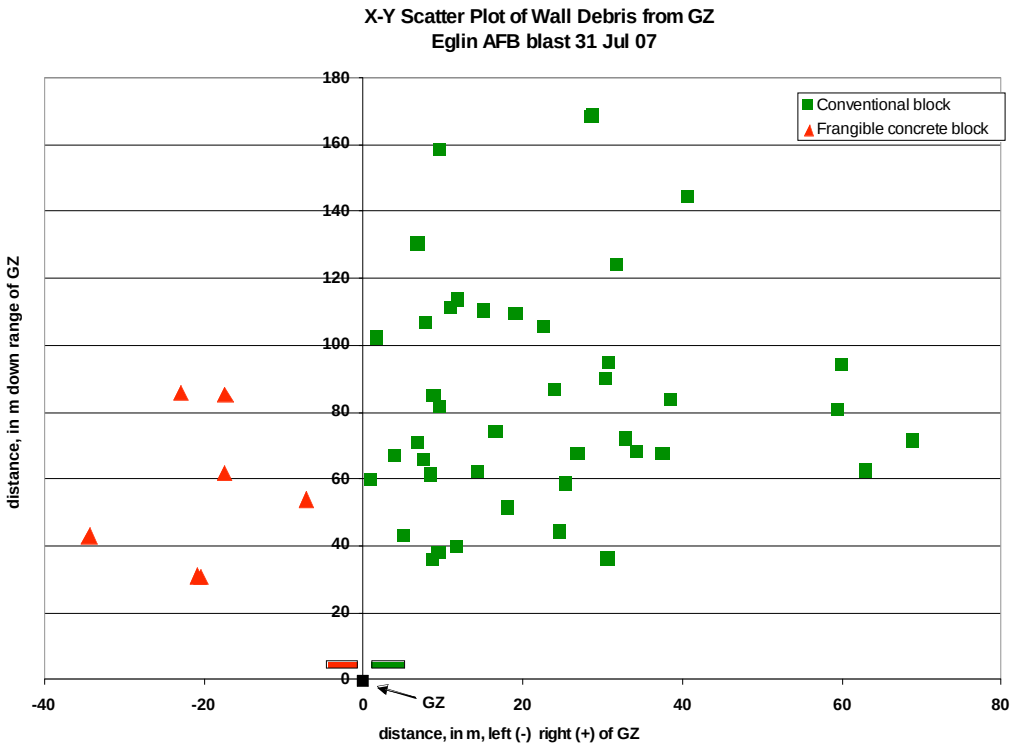

Fig. 11–X – Y scatter plot of wall debris from second field blast experiment.

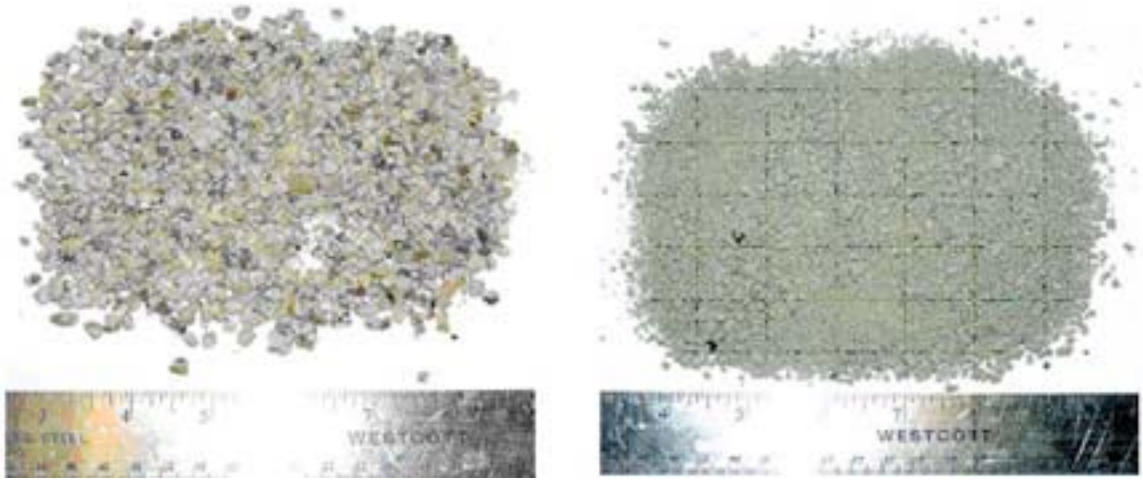

Fig. 12–Comparison of no-fines group (b), left and dense group (c), right.

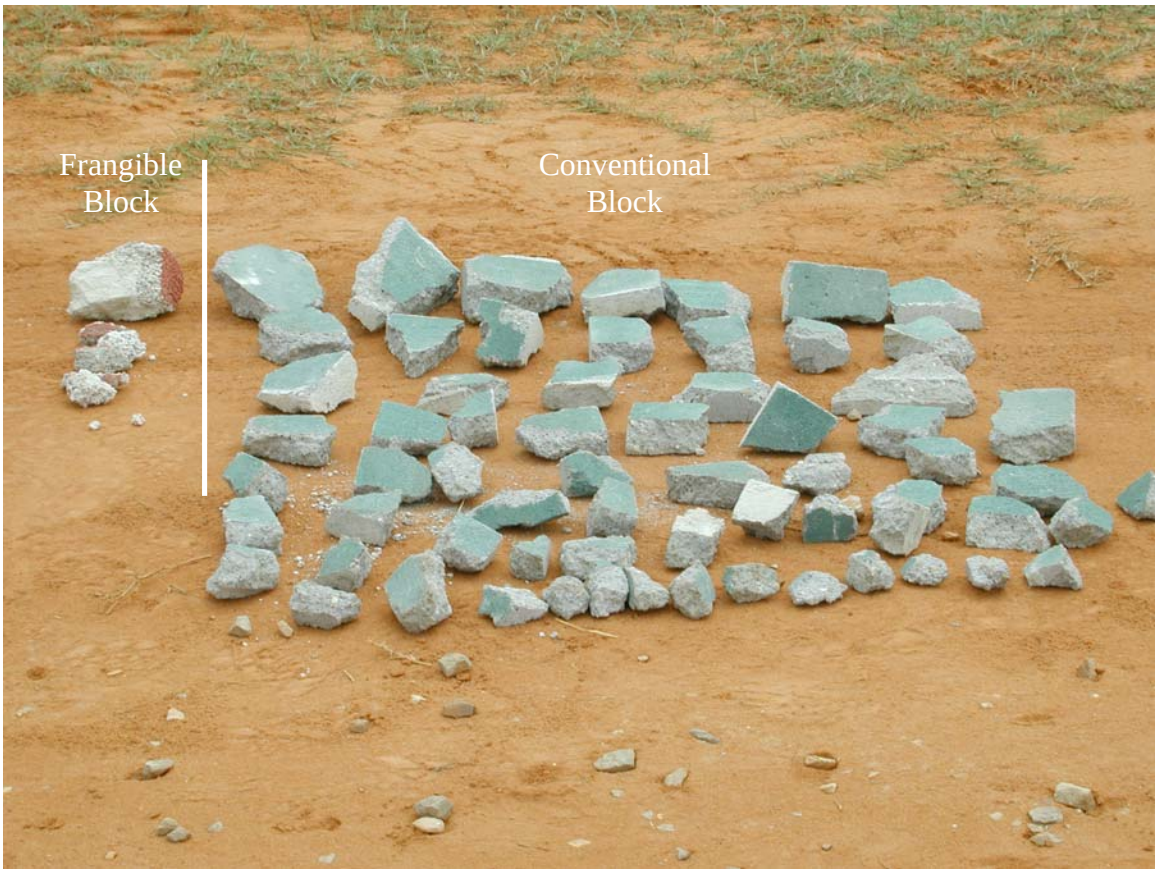

Fig. 13–Fragments collected from the second field blast.